ELSEVIER

Signal Processing: *Image Communication* 9 (1997) 159–169

SIGNAL PROCESSING: IMAGE COMMUNICATION

Image transmission over noisy channels using multicarrier modulation

Keang-Po Ho[a], Joseph M. Kahn[b,*]

[a] *Bellcore, 331 Newman Springs Road, Red Bank, NJ 07701, USA*

[b] *Department of Electrical Engineering and Computer Sciences, University of California, Berkeley, CA 94720, USA*

Received 18 July 1995

Abstract

We have proposed and analyzed a combined source–channel coding scheme using multicarrier modulation. By changing the power and modulation of subchannels carrying different bits of the compressed signal, the channel-induced distortion can be minimized. An algorithm for the subchannel power allocation is derived. As an example, for DCT- and subband-coded images, multicarrier systems using uncoded BPSK achieve more than a 9 dB improvement over single-carrier systems in terms of the image signal-to-distortion ratio on very noisy channels.

Keywords: Multicarrier modulation; Image coding; Channel coding; Source coding

1. Introduction

One of the most important results of Shannon's work was that source coding and channel coding can be treated separately without sacrificing fidelity [37, 38]. Traditionally, the source and channel codes are designed separately and then cascaded together. However, Shannon's argument is true only if both transmitter and receiver are permitted to have an infinite degree of complexity and infinite delay. In practice, because of channel-induced additive noise, the probability of bit error (bit-error rate, BER) is not infinitesimally small. In typical communication systems, in order to transmit an analog source, the source is quantized into binary bits and all bits are transmitted via the same channel, and are thus afforded the same protection against error. However, some bits in the quantized signal (e.g., the most significant bit) are far more important than others. In such a situation, we can combine the source and channel code into a single code, in which the objective is to minimize the overall distortion between the original source at the transmitter and its reconstruction at the receiver.

Multicarrier modulation, also referred to as orthogonal frequency division multiplexing (OFDM) or discrete multitone (DMT), is currently being considered as a standard channel-coding scheme for asymmetric digital subscriber lines (ADSL) and high-rate digital subscriber lines (HDSL) [2, 8], digital audio and high-definition television (HDTV) broadcasting [2, 11, 21] and wireless personal communication systems [9, 32]. Multicarrier modulation yields several important advantages over single-carrier systems [2]. In this

* Corresponding author. Tel.: (510) 643-8848; fax: (510) 642-2739; e-mail: jmk@eecs.Berkeley.EDU.

PII S0923-5965(96)00022-7

paper, we demonstrate an additional advantage of multicarrier modulation: it enables the use of combined source–channel coding in a natural way, without an increase in the complexity of either the transmitter or the receiver.

We will consider the use of multicarrier modulation to transmit discrete cosine transform (DCT)-coded and subband-coded images. First, the source encoder is fixed, and the importance of different quantized bits is evaluated. The different bits will be transmitted by different subchannels that provide different degrees of error protection, so as to minimize the overall distortion between the original signal at the transmitter and the reconstructed signal at the receiver. Usually, the overall distortion is the sum of the quantization distortion and the channel distortion [41]. For a fixed source encoder, the quantization distortion is given, and we seek to minimize the channel distortion using multicarrier modulation.

There are various schemes for combined source–channel coding or unequal error protection. According to the importance of each bit, codes with unequal error protection [14, 26] can be applied. Digital cellular [1], digital audio broadcasting [15], and digital television broadcasting [30] systems provide unequal error protection using different codes (or no code) for different classes of data. Another method to provide unequal error protection is the use of a multi-resolution constellation [5, 33, 46], either with or without coding. However, the number of classes of data is limited in most of the above methods, usually two or three classes. The achievable "granularity", or difference in error protection, is usually very large. By contrast, our multicarrier modulation system can provide a large number of different classes of error protection with arbitrarily fine "granularity".

The remainder of this paper is organized as follows. Section 2 discusses the channel-induced distortion and derives the weighting factors for different bits. Section 3 considers the transmission of DCT-coded images by multicarrier modulation systems. An algorithm for subchannel power allocation is derived. A numerical example is provided to show the improvement obtained by using multicarrier transmission. Section 4 describes the transmission of subband-coded images by multicarrier modulation systems. Sections 5 and 6 provide discussion and our conclusions, respectively.

[1] For example, the GSM system: European digital telecommunication system (phase 2); Channel coding (GSM 5.03), prETS 300 575, March 1995.

2. Channel-induced distortion

Our combined source–channel coding scheme uses a fixed source encoder and changes the channel modulation to minimize the channel-induced distortion. The source encoder consists of a DCT or subband transform followed by scalar quantizers. We employ optimal scalar quantizers designed by the method of Lloyd [24] and Max [27]. The quantizer partitions the real axis into Q regions of $(-\infty, x_1]$, $(x_i, x_{i+1}]$, $i = 1, 2, \ldots, Q-2$, $(x_{Q-1}, +\infty)$. Each region is quantized to the centroid of that region, y_i, $i = 0, 1, \ldots, Q-1$. For simplicity, we use natural binary coding, i.e., the codeword y_i is mapped to binary codeword i.

In the optimal scalar quantizer [24, 27], a codeword represents the centroid of the respective partition, so that the overall distortion from the original signal to the reconstructed signal is the sum of the quantization distortion and the channel-induced distortion [41]. The quantizer is given and fixed, and we seek to minimize the channel-induced distortion:

$$D_C = \sum_{i=0}^{Q-1} \sum_{j=0}^{Q-1} p_{y_i} P(j|i)\,(y_j - y_i)^2, \tag{1}$$

where p_{y_i} is a priori probability of codeword y_i, and $P(j|i)$ is the transition probability for transmission of binary codeword i and reception of binary codeword j.

The binary codewords are binary numbers of $n = \log_2 Q$ bits. Each bit is transmitted over a different subchannel using multicarrier modulation. The schematic diagram of a multicarrier modulation system is shown in Fig. 1. Each subchannel can utilize different power, modulation constellation, channel encoding, and carrier $\varphi_m(t)$, so that different error protection can be provided for different bits. The distortion between the original analog signal and the received signal can thereby be minimized. For a

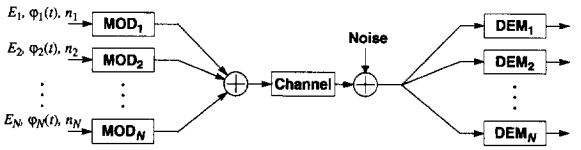

Fig. 1. Schematic diagram of a multicarrier system. E_m is the power transmitted in the mth subchannel, $\varphi_m(t)$ is the carrier of the mth subchannel, and n_m is the number of bits per symbol of the mth subchannel.

symbol time T, all carriers must be orthogonal to each other, or

$$\int_0^T \varphi_i(t)\varphi_j(t)\,\mathrm{d}t = \delta_{ij}. \tag{2}$$

The most popular multicarrier modulation systems use tones at different frequencies as carriers [2, 9, 18, 47]. A time-division multiplexed system can also be considered as a generalized multicarrier modulation system. Unequal error protection can be provided by using different constellations in each time slot.

Assuming that the BER of subchannel m is p_{b_m}, $m = 1, 2, \ldots, n$, the transition probabilities are

$$P(j|i) = \prod_{m=1}^{n} (1 - p_{b_m})^{1-l_m(i,j)} p_{b_m}^{l_m(i,j)}, \tag{3}$$

where $l_m(i,j) = 1$ if the binary codewords represented by i and j differ in the mth position and otherwise $l_m(i,j) = 0$. Usually, the BERs p_{b_m} are small, so that the probability of multiple bit errors within the same binary codeword is small, and any term having factors of $p_{b_{m1}} p_{b_{m2}}$, $m1, m2 = 1, 2, \ldots, n$, can be ignored. The transition probabilities are thus simplified to

$$P(j|i) = \begin{cases} 1, & i = j, \\ p_{b_m}, & l_m(i,j) = 1. \\ 0, & \text{otherwise.} \end{cases} \tag{4}$$

In this simplification, $P(j|i)$ is non-zero if i and j are equal, or are separated by a unit Hamming distance. For any n-bit binary number i, there are n different binary numbers separated from i by a Hamming distance of unity. If i_m is the mth bit in the binary representation of i, i.e., $i = \sum_{m=1}^{n} i_m 2^{n-m}$, those n binary numbers are

$$i_{e,m} = i + (1 - 2i_m)2^{n-m}, \quad m = 1, 2, \ldots, n. \tag{5}$$

After some algebra, the channel-induced distortion is found to be

$$D_C \approx \sum_{m=1}^{n} \sum_{i=0}^{Q-1} p_{b_m} p_{y_i} (y_{i_{e,m}} - y_i)^2 = \sum_{m=1}^{n} p_{b_m} w_{n,m}, \tag{6}$$

where

$$w_{n,m} = \sum_{i=0}^{Q-1} p_{y_i} (y_{i_{e,m}} - y_i)^2 \tag{7}$$

is the weighting factor of the mth bit. These weighting factors are the average mean-square error induced by a single bit error at position m of n-bit binary codewords.

The discrete cosine transform (DCT) coefficients and subband-transformed components can be described accurately as Laplacian-distributed random variables [3]. The Lloyd–Max quantizer for a Laplacian source can be easily designed by Method I of Lloyd [24]. Table 1 shows the weighting factors $w_{n,m}$ and other parameters of optimal scalar quantizers from one to nine bits for a zero-mean, unit-variance Laplacian source.

3. Discrete cosine transform coded images

The first operation of transform coding is a linear transformation that converts the set of statistically dependent random variables into a set of "more independent" coefficients. The optimal linear transformation is the Karhunen–Loeve (KL) transform [10], which results in independent coefficients. The KL transform has the property that it packs the maximum average energy into any reduced set of coefficients. However, the KL transform is difficult to implement because it is signal-dependent [16, 49]. The discrete cosine transform (DCT) is known to be a good approximation of the KL transform [6, 17], especially for highly correlated data. Because the two-dimensional (2-D) DCT has been shown to provide relatively efficient and robust performance in a variety of image coding applications, the 2-D DCT is employed in various international standards [28, 34] of still image and motion picture compression, including JPEG [31, 44], MPEG [7, 22] and H.261 [23].

Table 1
Parameters of the Lloyd–Max quantizer for unit-variance Laplacian source

Number of levels, Q	2	4	8	16	32	64	128	256	512
$w_{n,1}$ (dB)	3.010	7.058	9.520	11.122	12.173	12.856	13.296	13.576	13.754
$w_{n,2}$ (dB)		3.010	4.884	6.192	7.069	7.641	8.007	8.237	8.381
$w_{n,3}$ (dB)			−1.949	−0.867	−0.131	0.368	0.702	0.922	1.062
$w_{n,4}$ (dB)				−7.385	−6.798	−6.404	−6.143	−5.948	−5.824
$w_{n,5}$ (dB)					−13.098	−12.791	−12.586	−12.445	−12.347
$w_{n,6}$ (dB)						−18.960	−18.804	−18.699	−18.627
$w_{n,7}$ (dB)							−24.901	−24.822	−24.769
$w_{n,8}$ (dB)								−30.881	−30.842
$w_{n,9}$ (dB)									−36.882
MSE (dB)	−3.010	−7.540	−12.648	−18.133	−23.870	−29.743	−35.688	−41.671	−47.672

3.1. Subchannel power allocation

In image compression using the DCT, the image is divided into small blocks of size $p \times q$, and a 2-D DCT is employed for each small block. The variances of transform coefficient $\sigma_{k,l}^2$, $0 \leqslant k < p$, $0 \leqslant l < q$, can be estimated from the image or derived from the image model.

Assume that $n_{k,l}$ is the bit-allocation table determined by a bit-allocation algorithm [17, 35]. Assuming that the DCT coefficients are Laplacian distributed, if $w_{n,m}$ are the weighting factors of the mth bit of an n-bit optimal quantizer for unit-variance Laplacian source tabulated in Table 1, obviously, the weighting factors of the DCT coefficients are $\sigma_{k,l}^2 w_{n_{k,l},j}$. Let us assume that $p \times q$ 2-D DCT coefficients are quantized to a total of N bits and transmitted by an N-channel multicarrier modulation system. Assuming that a subchannel has a power of $E_{n_{k,l},j}$, the BER of that subchannel is a function of $E_{n_{k,l},j}$, or $p_{n_{k,l},j} = P_{n_{k,l},j}(E_{n_{k,l},j})$, where $P_\gamma(E)$ are the BER functions, which can be different for the individual subchannels if different modulation schemes and channel coding are employed. Therefore, we would like to minimize the channel-induced distortion per pixel:

$$D_C = \frac{1}{pq} \sum_{k=1}^{p} \sum_{l=1}^{q} \sum_{j=1}^{n_{k,l}} P_{n_{k,l},j}(E_{n_{k,l},j}) \sigma_{k,l}^2 w_{n_{k,l},j}, \tag{8}$$

with the constraint that the total power be equal to E_T. Using a Lagrange multiplier, the solution of (8) is

$$\sigma_{k,l}^2 w_{n_{k,l},j} G_{n_{k,l},j}(E_{n_{k,l},j}) = \lambda, \tag{9}$$

where $G_\gamma(E) = \mathrm{d}P_\gamma(E)/\mathrm{d}E$ is the derivative of $P_\gamma(E)$ with respect to the power E, and λ is the Lagrange multiplier. For a fixed overall power, the multiplier λ can be found by solving

$$\sum_{k=1}^{p} \sum_{l=1}^{q} \sum_{j=1}^{n_{k,l}} G_{n_{k,l},j}^{-1}(\lambda/(\sigma_{k,l}^2 w_{n_{k,l},j})) = E_T, \tag{10}$$

where $G_\gamma^{-1}(E)$ are the inverse functions of $G_\gamma(E)$. Although complicated, the nonlinear equation (10) is a one-variable equation that can be solved easily by simple numerical methods.

3.2. Numerical example

In order to provide a simple numerical example, we consider images transmitted over an AWGN channel, and we assume that all subchannels are identically modulated using binary phase-shift keying (BPSK). The BER function is $p_b = \frac{1}{2}\mathrm{erfc}(\sqrt{\rho})$, where $\rho = E/\sigma_n^2$ is the signal-to-noise ratio (SNR) of the subchannel and σ_n^2 is the variance of Gaussian noise in the subchannel. For a Gaussian channel, the function $G_\gamma(E)$ is a monotonic function so that the expression (10) can be solved by a simple bisection method.

The original 256 gray-scale Lena image shown in Fig. 2 is employed for a demonstration. First, 128 is subtracted from the image, and then the image is divided into small square blocks of size 16 × 16. The 2-D DCT is computed for each block and the

Fig. 2. The original gray-scale image of Lena.

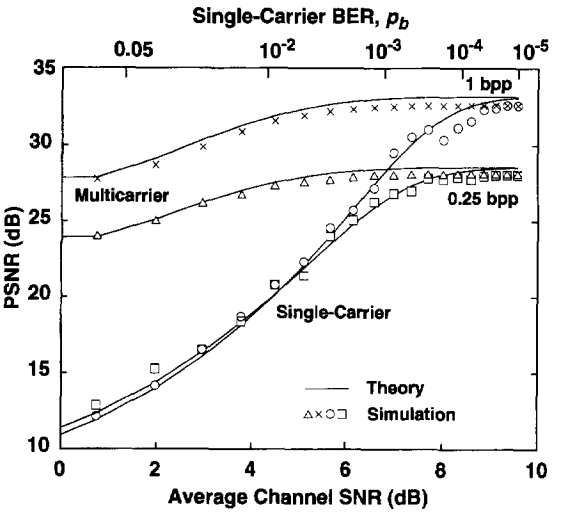

Fig. 3. PSNR as a function of average SNR of the channel and single-channel BER for a DCT-coded image. Both theoretical and simulation results are shown for comparison.

variances of the DCT coefficients are estimated. The transform coefficients are normalized by their standard deviation $\sigma_{k,l}$ and quantized by the optimal quantizer for a unit-variance Laplacian distribution using fixed-length quantizer. The bit allocation is determined by the integer bit-allocation algorithm [17, 35].

Fig. 3 shows the peak signal-to-noise ratio (PSNR) as a function of average SNR of the channel, and the corresponding BER of the single-carrier system. The average SNR of the channel is the total power divided by the total noise variance of all subchannels. In Fig. 3, the image is compressed to both 0.25 bpp (bit/pixel) and 1 bpp. Both theoretical results computed using expression (8) and simulation results are shown for comparison. The difference between the theoretical and simulation PSNR is smaller than 0.8 dB, allowing us to infer the validity of both the Laplacian distribution and the approximation of the transition probabilities (4). For high channel SNRs, the PSNR of single-carrier and multicarrier systems are identical because the BER is small and the quantization distortion is much larger than the channel-induced distortion.

For low channel SNRs, the PSNR of the multicarrier system is much larger than that of the single-carrier system. At SNRs less than 3 dB, the improvement in PSNR of the multicarrier over the single-carrier system is more than 9.5 dB for the 0.25-bpp image and more than 13.5 dB for the 1-bpp image. Alternatively, the average channel SNR required to achieve a specified PSNR in a multicarrier system is much smaller than for a single-carrier system. For PSNR degradations more than 1 dB (i.e., the PSNR is at least 1 dB smaller than on the noiseless channel), the gain in average channel SNR ranges from 3.5 to 5.5 dB for average channel SNRs larger than 2 dB.

Fig. 4 shows the image compressed to 0.25 bpp and the corresponding integer bit-allocation table. The PSNR of the image is 28.05 dB. From the bit-allocation table, we see that only 25 coefficients are used in the 0.25-bpp compressed image. Fig. 3.2 compares the images transmitted over single-carrier and multicarrier systems for SNR = 4.32 dB, which corresponds to a single-carrier BER of $p_b = 10^{-2}$. A 6.5-dB improvement in PSNR is achieved by use of multicarrier modulation. While channel errors cause the PSNR of the image transmitted over the single-carrier system to degrade by 7.5 dB to 20.52 dB, that of the multicarrier system degrades by only 1 dB to 27.01 dB.

7	5	4	3	2	2	1	0	0	0	0	0	0	0	0	0
4	4	3	3	2	1	0	0	0	0	0	0	0	0	0	0
3	3	3	2	1	1	0	0	0	0	0	0	0	0	0	0
2	2	2	2	1	0	0	0	0	0	0	0	0	0	0	0
0	0	0	1	0	0	0	0	0	0	0	0	0	0	0	0
0	0	0	0	0	0	0	0	0	0	0	0	0	0	0	0
0	0	0	0	0	0	0	0	0	0	0	0	0	0	0	0
0	0	0	0	0	0	0	0	0	0	0	0	0	0	0	0
0	0	0	0	0	0	0	0	0	0	0	0	0	0	0	0
0	0	0	0	0	0	0	0	0	0	0	0	0	0	0	0
0	0	0	0	0	0	0	0	0	0	0	0	0	0	0	0
0	0	0	0	0	0	0	0	0	0	0	0	0	0	0	0
0	0	0	0	0	0	0	0	0	0	0	0	0	0	0	0
0	0	0	0	0	0	0	0	0	0	0	0	0	0	0	0
0	0	0	0	0	0	0	0	0	0	0	0	0	0	0	0
0	0	0	0	0	0	0	0	0	0	0	0	0	0	0	0

Fig. 4. The DCT-coded image of 0.25 bpp and the integer bit allocation table. The PSNR of the image is 28.05 dB.

(a) Single-Carrier **(b) Multicarrier**

Fig. 5. Decoded DCT-coded image at the receiver of single-carrier and multicarrier systems. The average SNR of the channel is 4.32 dB, corresponding to a single-carrier BER of $p_b = 10^{-2}$. (a) Transmitted through a single-carrier system, PSNR = 20.52 dB. (b) Transmitted through a multicarrier system, PSNR = 27.01 dB.

4. Subband-coded images

Subband coding has been shown to be an efficient technique for image coding [1, 20, 25, 43, 48, 50]. Subband pyramids [1, 25, 36], which combine the ideas behind subband coding and pyramid coding [4, 45], can more fully utilize the image correlation in low-frequency subbands than other image compression methods. Recursive subband decomposition can be considered as a fast implementation of the discrete wavelet transform, which has generated considerable interest for various applications recently [25]. The subband pyramid itself splits an image into a hierarchy of bandpass components. Each of these components has better energy compaction than the original image.

For the simplest possible subband decomposition of a one-dimensional signal, a signal is passed through a high-pass filter and a low-pass filter, and the outputs of these two filters are subsampled by a factor of two, as shown in Fig. 6. For upsampling and reconstruction, a low-pass and a high-pass filter are used, and their outputs are combined to yield the reconstructed signal. The filters must be chosen in the correct way, so that the aliasing provided by the 2 : 1 subsampling cancels out in the reconstruction and upsampling process. Quadrature mirror filters (QMFs) [42, 43] are usually employed for two-band subband decomposition. The frequency responses of the high-pass and the low-pass filter are mirror images of each other. Identical high-pass and the low-pass filters are used for the analysis and the synthesis filter banks.

We adopt a subband decomposition scheme illustrated in Fig. 7. On each pyramid level, the low band is decomposed into four subbands by the operation of a horizontal and vertical 2 : 1 band splitting using 2-D separable QMFs. The low-pass and high-pass QMFs are identical to those used in [36]. The resulting four subbands are a horizontal high band, a vertical high band, a diagonal high band, and a new low band. Because an odd number of taps in the QMFs is used, these filters require that the subsampling points be staggered between the two subbands, i.e., the subsampling points of low-pass and high-pass filter need to be offset by one pixel. This alternating sampling preserves the information more uniformly. As adjacent image samples have a large positive correlation, most of the energy is concentrated in the low band. The energy contained in other subbands is usually much smaller.

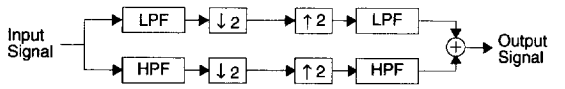

Fig. 6. Subband decomposition and reconstruction of a signal.

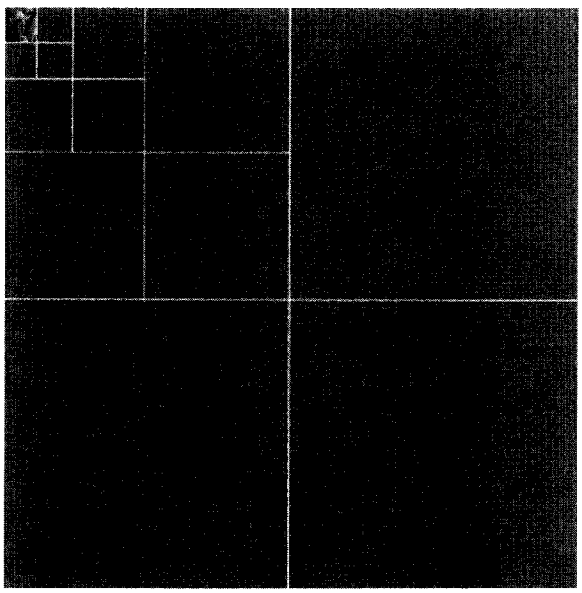

Fig. 7. Four-level subband pyramid decomposition of the image of Lena in Fig. 2.

Zero pads can be placed at the edge of images for the convolution of the image with the QMFs. However, zero pads generate 'ringing' at the edge of the image. To prevent this ringing, the reflection of the image is placed at the edge of the image, i.e., in our case, the fifth, fourth, third and second columns of the image are placed before the first column of the image in consecutive order. Usually, the QMFs are symmetric so that the convolved image is still symmetric with respect to the edge, therefore, this process does not increase the number of samples in the subband decomposition.

The lowest subband is usually coded by differential pulse code modulation (DPCM) [1, 12, 50] or vector quantization [36, 48]. Other subbands can be coded

Fig. 8. Subband coded image of rate 0.25 bpp. The PSNR of the image is 29.24 dB.

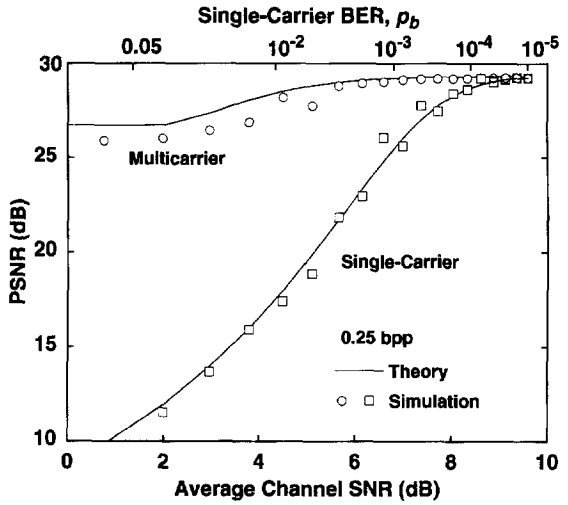

Fig. 9. PSNR as a function of average SNR of the channel and single-channel BER for a subband-coded image. Both theoretical and simulation results are shown for comparison.

using DPCM [50], PCM [12] or vector quantization [36, 48]. For simplicity, we code the lowest subband using DPCM and other subbands using PCM. Each subband component is quantized by the optimal Lloyd–Max quantizer for a Laplacian source, as described in Table 1.

Fig. 8 shows subband coded image of Lena at a rate of 0.25 bpp. The PSNR of the image is 29.24 dB, which is about 2 dB larger than that of Fig. 4, which used DCT. In addition, a subband-coded image does not have the blocking effect of a DCT-coded image, because the subband transform operates on the whole image, whereas the DCT operates on small blocks of the image. Subband-coded images also provide progressive and scalable image transmission in a natural way [13, 39, 40] so that the low subband can be transmitted first to produce a low-resolution image. The high subbands can be transmitted later to enhance the image, or not transmitted at all, thus providing scalable transmission. The subband-coded image can be transmitted by multicarrier modulation systems using the combined source–channel coding scheme. The power-allocation algorithm is similar to that of Section 3. The goal is to minimize the channel-induced distortion due to bit errors of the channel.

Fig. 9 shows the PSNR as a function of the average SNR of the channel, and the corresponding BER of the single-carrier system. The image is compressed to 0.25 bpp. Both the theoretical results and simulation results are shown for comparison. The difference between the theoretical and simulation PSNR is small, especially for the single-carrier case. Similar to the results of Fig. 3, at high channel SNRs, the PSNR of single-carrier and multicarrier systems are identical, because the BER is low and the quantization distortion is dominant.

For average channel SNRs less than 8 dB, the channel-induced distortion becomes observable for the single-carrier system and degrades the PSNR of the image. The PSNR of the multicarrier system degrades much more slowly than that of the single-carrier system. For low channel SNRs, the PSNR of the multicarrier system is much larger than that of the single-carrier system. At SNRs less than 3 dB, the improvement of the multicarrier over the single-carrier system is more than 10 dB. In order to achieve a given PSNR, the average SNR required in the multicarrier system is 3–5 dB less than for the single-carrier system for PSNRs less than 28 dB.

Fig. 10 compares the images transmitted over a single-carrier and a multicarrier system for SNR = 4.32 dB, which corresponds to a single-carrier BER of $p_b = 10^{-2}$. An 11-dB improvement in PSNR is

Fig. 10. Decoded subband-coded image at the receiver of single-carrier and multicarrier systems. The average SNR of the channel is 4.32 dB, corresponding to a single-carrier BER of $p_b = 10^{-2}$. (a) Transmitted through single-carrier system, PSNR = 16.41 dB. (b) Transmitted through multicarrier system, PSNR = 28.09 dB.

achieved by the use of multicarrier modulation. While channel errors cause the PSNR of the image transmitted over the single-carrier system to degrade by more than 12.5 dB to a PSNR of 16.41 dB, that of multicarrier system degrades by only 1.25 dB to 28.09 dB.

5. Discussion

In a practical implementation on a channel having limited bandwidth, multilevel modulation will be used for the digital transmission. Results of both the Figs. 3 and 9 can be modified easily for M-ary QAM or VSB systems. For example, with coherent demodulation, the BER formula for an M-ary QAM system is $p_b = K\,\mathrm{erfc}(\sqrt{\rho/\alpha})$, where K and α are constants that depend on the number of levels M. For M ranging from 2 (BPSK) to 1024, the value of K lies between $\frac{1}{2}$ and $\frac{1}{4}$. To a good approximation, the x-axis of Figs. 3 and 9 can simply be shifted right by $10\log_{10}(\alpha)$ dB for an M-ary QAM system.

In Sections 3 and 4, for simplicity, we presented numerical examples using uncoded BPSK. A practical implementation is likely to use error-correction coding as part of the channel-coding scheme. Our subchannel power allocation scheme, described in Section 3.1, is general enough to permit different subchannels to have different BER functions, which might be achieved using different modulation schemes and/or error-correction codes on different subchannels. Here, we provide an example illustrating the PSNR gains that can be achieved using two different modulation schemes, in addition to power allocation, to provide unequal error protection.

We consider an image DCT-coded to 0.25 bpp in a manner identical to that in Fig. 3. The coded bits are divided into two groups according to their importance. The more important bits are transmitted by BPSK modulation, and the less important ones are transmitted using QPSK modulation. Thus, two-thirds of the channels utilize BPSK, and one-third use QPSK. This system occupies $\frac{3}{4}$ the bandwidth of an all-BPSK system. Fig. 11 shows the PSNR versus SNR for this example. In the unequal-power case, the power is allocated to the various BPSK and QPSK channels according to the power-allocation scheme of Section 3.1. For comparison purposes, we also consider the equal-power case, in which all

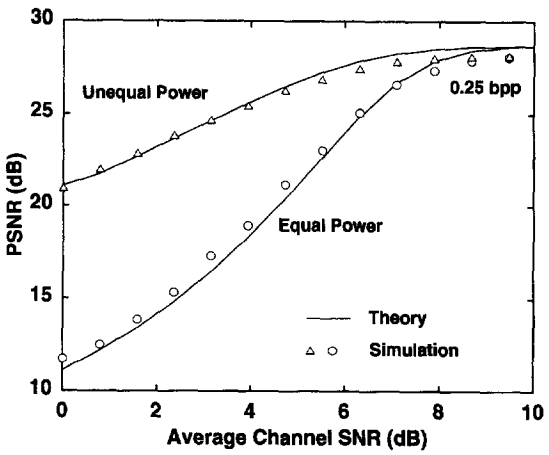

Fig. 11. PSNR as a function of average channel SNR for a DCT-coded image. Half of the bits are transmitted by BPSK modulation and half of the bits are transmitted by QPSK modulation. Both theoretical and simulation results are shown for comparison.

BPSK and QPSK channels have the same SNR. We note that for a fixed symbol rate, BPSK requires a 3-dB lower SNR than QPSK to achieve a given BER.

Comparing the PSNRs in Figs. 3 and 11, there is almost no difference between the single-carrier system in Fig. 3 and the equal-power case in Fig. 11. This is because there are some "very" important bits, and errors in these bits dominate the PSNR performance of the system (our numerical results indicate that the importance of the bits ranges over three to four orders of magnitude). Comparing Figs. 3 and 11, in the case of unequal carrier powers, the results of Fig. 11 are 1–3 dB worse at a given SNR. In Fig. 11, the use of unequal carrier powers yields a PSNR improvement over the equal-power case of more than 9 dB at low SNRs.

6. Conclusions

A combined source–channel coding scheme using multicarrier modulation is proposed and analyzed for DCT- and subband-coded images. Allocation of subchannel powers according to the importance of each bit achieves a large improvement in PSNR over single-carrier modulation. A numerical example shows that on very noisy channels, multicarrier systems using uncoded BPSK can achieve an improvement over single-carrier systems of more than 9 dB in terms of image signal-to-distortion ratio. The result here for subband-coded images can be extended easily to video coding using 3-D subband coding [20, 29, 40].

Acknowledgements

The authors would like to thank Prof. M. Vetterli for helpful discussions. This research has been funded by National Science Foundation Presidential Young Investigator Award ECS-9157089 and The Hughes Aircraft Company.

References

[1] E.H. Adelson, E. Simoncelli and R. Hingorani, "Orthogonal pyramid transforms for image coding", *Visual Communications and Image Processing II, Proc. SPIE*, Vol. 845, 1987, pp. 50–58.

[2] J.A.C. Bingham, "Multicarrier modulation for data transmission: an idea whose time has come", *IEEE Commun. Mag.*, May 1990, pp. 5–14.

[3] K.A. Birney and T.R. Fischer, "On the modeling of DCT and subband image data for compression", *IEEE Trans. Image Processing*, Vol. 4, 1995, pp. 186–193.

[4] P.J. Burt and E.H. Adelson, "The Laplacian pyramid as a compact image code", *IEEE Trans. Commun.*, Vol. 31, 1983, pp. 532–540.

[5] A.R. Calderbank and N. Seshadri, "Multilevel codes for unequal error protection", *IEEE Trans. Inform. Theory*, Vol. 39, 1993, pp. 1234–1248.

[6] W.-H. Chen and C.H. Smith, "Adaptive coding of monochrome and color images", *IEEE Trans. Commun.*, Vol. COM-25, 1977, pp. 1285–1292.

[7] L. Chiariglione, "The development of an integrated audio-visual coding standard: MPEG", *IEEE Proc.*, Vol. 83, 1995, pp. 151–157.

[8] J.S. Chow, J.C. Tu and J.M. Cioffi, "A discrete multitone transceiver system for HDSL applications", *IEEE J. Select. Areas Commun.*, Vol. 9, 1991, pp. 895–908.

[9] L.J. Cimini, Jr., "Analysis and simulation of a digital mobile channel using orthogonal frequency division multiplexing", *IEEE Trans. Commun.*, Vol. COM-33, 1985, pp. 665–675.

[10] W.B. Davenport, Jr. and W.L. Root, *An Introduction to the Theory of Random Signals and Noise*, McGraw Hill, New York, 1958, pp. 96–99.

[11] T. de Couason, R. Monnier and J.B. Rault, "OFDM for digital TV broadcasting", *Signal Processing*, Vol. 39, Nos. 1–2, September 1994, pp. 1–32.

[12] H. Gharavi and A. Tabatabai, "Sub-band coding of monochrome and color image", *IEEE Trans. Circuits Systems*, Vol. 35, 1988, pp. 207–214.

[13] B. Girod, "Scalable video for multimedia workstations", *Comput. Graph.*, Vol. 17, 1993, pp. 269–276.

[14] J. Hagenauer, "Rate-compatible punctured convolutional codes (RCPC codes) and their applications", *IEEE Trans. Commun.*, Vol. COM-36, 1988, pp. 389–400.

[15] P. Hoeher, J. Hagenauer, E. Offer, C. Rapp and H. Schuze, "Performance of an RCPC-coded OFDM-based digital audio broadcasting (DAB) system", in: *IEEE GLOBECOM '91*, Phoenix, AZ, 1991, pp. 2.1.1–2.1.7.

[16] A.J. Jain, "Image data compression: A review", *Proc. IEEE*, Vol. 69, 1981, pp. 349–389.

[17] A.J. Jain, *Fundamentals of Digital Image Processing*, Prentice-Hall, Englewood Cliffs, NJ, 1989, pp. 501–504.

[18] I. Kalet, "The multitone channel", *IEEE Trans. Commun.*, Vol. 37, 1989, pp. 119–124.

[19] K.D. Kammeyer, U. Tuisel, H. Schulze and H. Bockmann, "Digital multicarrier-transmission of audio signals over mobile radio channels", *European Trans. Telecommun. Related Technol.*, Vol. 3, 1992, pp. 243–253.

[20] G. Karlsson and M. Vetterli, "Three dimensional sub-band coding of video", *Proc. Internat. Conf. Acoust. Speech Signal Process. '88*, Vol. 2, 1988, pp. 1100–1103.

[21] B. Le Floch, M. Alard and C. Berrou, "Coded orthogonal frequency division multiplex", *Proc. IEEE*, Vol. 83, 1995, pp. 982–996.

[22] D. Le Gall, "MPEG: A video compression standard for multimedia applications", *Commun. ACM*, Vol. 34, April 1991, pp. 46–58.

[23] M.L. Liou, "Visual telephony as an ISDN application", *IEEE Commun. Mag.*, Vol. 28, February 1990, pp. 30–38.

[24] S.P. Lloyd, "Least squares quantization in PCM", Bell Laboratories Technical Note, 1957, published in *IEEE Trans. Inform. Theory*, Vol. IT-28, 1982, pp. 129–137.

[25] S.G. Mallat, "Multifrequency channel decompositions of images and wavelet models", *IEEE Trans. Acoust. Speech Signal Process.*, Vol. ASSP-37, 1989, pp. 2091–2110.

[26] B. Masnick and J. Wolf, "On linear unequal error protection codes", *IEEE Trans. Inform. Theory*, Vol. IT-13, 1967, pp. 600–607.

[27] J. Max, "Quantizing for minimum distortion", *IRE Trans. Inform. Theory*, Vol. IT-6, March 1960, pp. 7–12.

[28] A.N. Netravali and B.G. Haskell, *Digital Pictures: Representation, Compression and Standards*, Plenum Press, New York, 1995, 2nd edition, Chapter 7–9, pp. 571–640.

[29] K.N. Ngan and W.L. Chooi, "Very low bit rate video coding using 3D subband approach", *IEEE Trans. Circuits Systems Video Technol.*, Vol. 4, 1994, pp. 309–316.

[30] J. Palicot and J. Veillard, "Possible channel coding and modulation system for the satellite broadcasting of a high-definition television signal", *Signal Processing: Image Communication*, Vol. 5, Nos. 5–6, December 1993, pp. 463–471.

[31] W.B. Pennebaker and J.L. Mitchell, *JPEG Still Image Data Compression Standard*, Van Nostrand Reinhold, New York, 1992.

[32] C. Petrovic, W. Roehr and D.W. Cameron, "Multicarrier modulation for narrowband PCS", *IEEE Trans. Vehicular Technol.*, Vol. 43, 1994, pp. 856–862.

[33] K. Ramchandran, A. Ortega, K.M. Uz and M. Vetterli, "Multiresolution broadcast for digital HDTV using joint source/channel coding", *IEEE J. Select. Areas in Commun.*, Vol. 11, 1993, pp. 6–23.

[34] R. Schafer and T. Sikora, "Digital video coding standards and their role in video communications", *Proc. IEEE*, Vol. 83, 1995, pp. 907–924.

[35] A. Segall, "Bit allocation and encoding for vector sources", *IEEE Trans. Inform. Theory*, Vol. IT-22, 1976, pp. 162–169.

[36] T. Senoo and B. Girod, "Vector quantization for entropy coding of image subbands", *IEEE Trans. Image Processing*, Vol. 1, 1992, pp. 526–532.

[37] C.E. Shannon, "A mathematical theory of communication", *Bell System Tech. J.*, Vol. 27, 1948, pp. 379–423, 623–656.

[38] C.E. Shannon, "Coding theorems for a discrete source with a fidelity criterion", *IRE Nat. Conv. Rec.*, March 1959, pp. 142–163.

[39] A. Singh and V.M. Bove, Jr., "Multidimensional quantizers for scalable video compression", *IEEE J. Select. Areas Commun.*, Vol. 11, 1993, pp. 36–45.

[40] D. Taubman and A. Zakhor, "Multirate 3-D subband coding of video", *IEEE Trans. Image Processing*, Vol. 3, 1994, pp. 572–588.

[41] R.E. Totty and G.C. Clark, "Reconstruction error in waveform transmission", *IEEE Trans. Inform. Theory*, Vol. IT-13, 1967, pp. 336–338.

[42] P.P. Vaidyanathan, *Multirate Systems and Filter Banks*, Prentice-Hall, Englewood Cliffs, NJ, 1993.

[43] M. Vetterli, "Multi-dimensional sub-band coding: some theory and algorithms", *Signal Processing*, Vol. 6, No. 2, April 1984, pp. 97–112.

[44] G.K. Wallace, "The JPEG still picture compression standard", *Commun. ACM*, Vol. 34, April 1991, pp. 30–44.

[45] L. Wang and M. Goldberg, "Progressive image transmission using vector quantization on images of pyramid form", *IEEE Trans. Commun.*, Vol. 37, 1989, pp. 1339–1349.

[46] L.-F. Wei, "Coded modulation with unequal error protection", *IEEE Trans. Commun.*, Vol. 41, 1993, pp. 1439–1449.

[47] S.B. Weinstein and P.M. Ebert, "Data transmission by frequency-division multiplexing using the discrete Fourier transform", *IEEE Trans. Commun. Tech.*, Vol. COM-19, 1971, pp. 628–634.

[48] P.H. Westerink, D.E. Boekee, J. Biemod and J.W. Woods, "Subband coding of images using vector quantization", *IEEE Trans. Commun.*, Vol. 36, 1988, pp. 713–719.

[49] P.L. Wintz, "Transform picture coding", *Proc. IEEE*, Vol. 60, 1972, pp. 800–820.

[50] J.W. Woods and S. D. O'Nell, "Subband coding of images", *IEEE Trans. Acoust. Speech Signal Process.*, Vol. ASSP-34, 1986, pp. 1278–1288.